13th World Conference on Earthquake Engineering
Vancouver, B.C., Canada
August 1-6, 2004
Paper No. 402

# SHAKING TABLE TEST OF REINFORCED CONCRETE FRAMES FOR VERIFICATION OF SEISMIC STRENGTHENING WITH POLYESTER SHEET

**Toshimi KABEYASAWA[1], Shun'ichi IGARASHI[2], YouSok KIM[3]**

## SUMMARY

A new method of strengthening reinforced concrete columns, named as SRF, has been developed and verified through a series of static column tests. Through these test series, the method has been improved to be effective to prevent the loss of capacity not only against axial load but also against lateral load reversals. In addition, a dynamic test was planned and conducted for the verification of the effectiveness of the new strengthening method, especially on the ultimate structural safety. The specimens are two one-third scale reinforced concrete wall-frame structures with considerable stiffness and strength eccentricity in the first story. The two specimens with the same sectional dimensions and reinforcement details were constructed and tested simultaneously on the large shaking table at NIED, Tsukuba. One was a bare reinforced concrete structure designed following old practice on reinforcement details in Japan, while the other was strengthened before the test with polyester fiber sheet, called as SRF. The torsional response in the first story magnified the displacement of the independent columns on the weak side row due to the large eccentricity, and these two columns without strengthening failed in shear resulting in collapse associated with loss of the axial load carrying capacity, whose collapse process was traced on the basis of test results. On the other hand, the frame strengthened by SRF not only responded stably to the same input motion with minor damage but also survived still higher levels of succeeding input motions. The cost of retrofit by SRF would remarkably be reduced from that by existing technology.

## INTRODUCTION

A lot of casualties have been caused due to the collapse of building structures even by recent major earthquakes in the countries with advanced earthquake engineering technologies. Although research themes in earthquake engineering are being oriented to innovative technology for new structures, continuous efforts are still important to reduce loss-of-life by developing an economical way of retrofit for existing buildings. To prevent the casualties due to structural failure during major earthquakes, it is primarily important to maintain the gravity load carrying capacity even in the cases that the response

[1] Professor, Earthquake Research Institute, The University of Tokyo, Japan. Email: kabe@eri.u-tokyo.ac.jp
[2] President, Square Inc., Japan. Email: igarashi.shunichi@sqa.co.jp
[3] Graduate Student, Earthquake Research Institute, The University of Tokyo, Japan, Email: yskim@eri.u-tokyo.ac.jp

would exceed the limit state expected from design earthquake intensity. In some cases of old reinforced concrete buildings, the columns would lose the capacity due to inadequate amount of confining hoops or shear reinforcement, then the buildings would collapse in the weak story or totally like so-called pancake. The development of an economical and simple strengthening method would be very worthwhile to prevent these brittle columns from the gravity load collapse during strong earthquake. A new method of strengthening reinforced concrete columns against axial failure was developed and verified through seismic tests on columns. The purpose of the strengthening was specially focused on the maintenance of axial load capacity of the columns until the excessive lateral deformation in the first stage, although the lateral load capacity could also be improved(Kabeyasawa [1[[2]]. A dynamic test was planned and conducted for the verification of the effectiveness of the new strengthening method, especially on the ultimate structural safety(Kabeyasawa[3][4]). The results of the shaking table test are presented in this paper.

## SPECIMENS

A one-third scale reinforced concrete specimen was used in this experiment, which comprises wall and column frame in the first story and wall frames only in the second story as shown in Figure 1. The cross-sectional dimensions and details of wall and column are illustrated in Table 1.

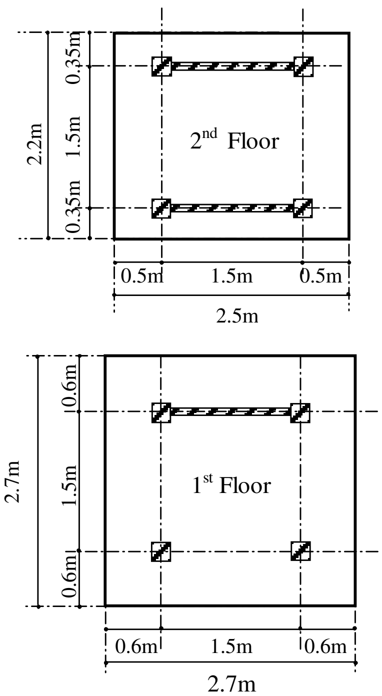


**Figure 1 Plan of specimen**

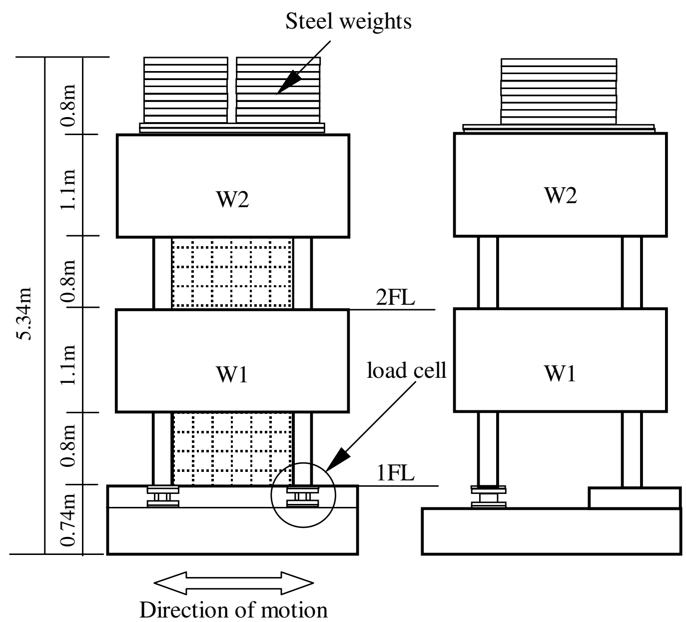


**(a) view from south** **(b) view from east**

**Figure 2 Elevation of specimen**

Total height of specimen is 5340mm, which is the sum of base (500mm), load cell (240mm), the first story (800mm), W1 (1100mm), the second story (800mm), W2 (1100mm) and steel plates (800mm) (Figure 2). Two concrete masses, W1 and W2 (284.6 $KN$), and steel plates (148.3 $KN$) on the specimen produced axial load stress, 0.15 $A_g f_c$ ( $f_c = 18MPa$ ) in the first story column, which corresponded to that of six-story building. The first story independent columns were designed following 1970's Japanese reinforcement detail practice, which could be vulnerable to shear failure after flexural yielding, as shown in Figure 3.

**Table 1: Section details of members**

| Floor | Column | | Wall | |
|---|---|---|---|---|
| 2 | X×Y | 200×200 | Thickness | 50 |
| | Main bar | 12-D10 | Vertical and horizontal bar | D6@100 |
| | Hoop | 2-D6@50 | | |
| 1 | X×Y | 200×200 | Thickness | 50 |
| | Main bar | 12-D10 | Vertical and horizontal bar | D6@100 |
| | Hoop | 2-D4@50 | | |

**Table 2: Material properties of concrete**

| | $\sigma_B$ (MPa) | $\varepsilon_c$ ($\mu$) | $E_c$ (MPa) | $\sigma_t$ (MPa) | age (days) |
|---|---|---|---|---|---|
| Superstructure | 24.1 | 1894 | 21556 | 2.38 | 86 |
| Base | 25.37 | 2060 | 23096 | 2.22 | 108 |

**Table 3: Material properties of steels**

| | $E_s$ (MPa) | $\sigma_y$ (MPa) | $\varepsilon_y$ ($\mu$) |
|---|---|---|---|
| D4 | 156490 | 188.4 | 1210 |
| D6 | 185288 | 439.1 | 2372 |
| D10 | 175137 | 352.4 | 2011 |

**Table 4: Stiffness and strength eccentricity ('( )' indicate shear coefficient)**

| | Column side | Wall side |
|---|---|---|
| Elastic stiffness ($N/mm$) | $9.1\times10^4$ | $4.57\times10^5$ |
| Strength ($KN$) | 125.5 (0.28) | 429.7 (0.97) |
| Base shear coefficient | 1.25 | |
| Stiffness eccentricity | 0.24 | |
| Strength eccentricity | 0.25 | |

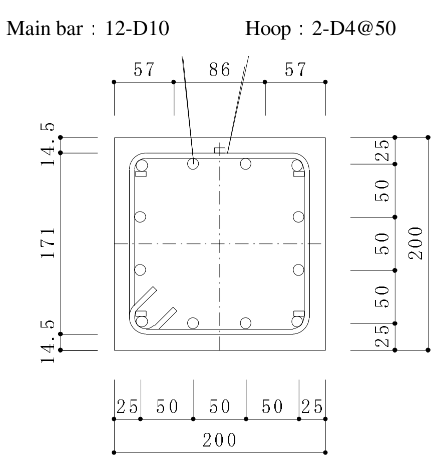


**Figure 3 reinforcement details of column**

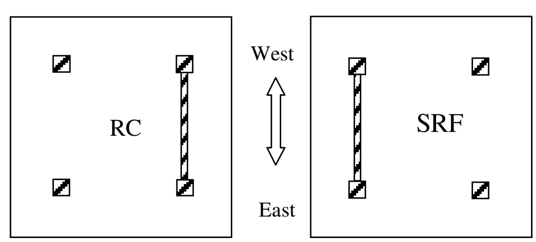


**Figure 4 Specimen arrangement on shake table**

## STRENGTHENING METHOD

Two specimens with the same properties and dimension were constructed and tested on the shake table simultaneously as shown in Figure 4, one of which was strengthened with polyester fiber sheet and belt (SRF specimen) and the other was not (RC specimen). The polyester sheet used for reinforcing materials in this experiment was developed to improve the capability of vertical member sustaining axial load under large lateral deformation caused by severe earthquake loading, whose effectiveness had been verified through the static column tests with various conditions([1][2]). The characteristics of the sheet are such as toughness, durability, heat-resistance and flexibility, which improve workability and need no special technique in reinforcing process. The properties of SRF sheet and belt are summarized in Table 5 and the results of tensile test showed almost linear relationship between stress-strain relations, and the sheet failed at relatively large strains of 0.10 to 0.35. Only the first story in the SRF specimen was reinforced. The reinforcing method and materials are a little different in column and wall side. Column side was wrapped with 3mm single-layer polyester belt (Figure 5(a)), while the wall with boundary columns were wrapped with double layer polyester sheet of 0.9mm, using epoxy-urethane adhesive (Figure 5(b)).

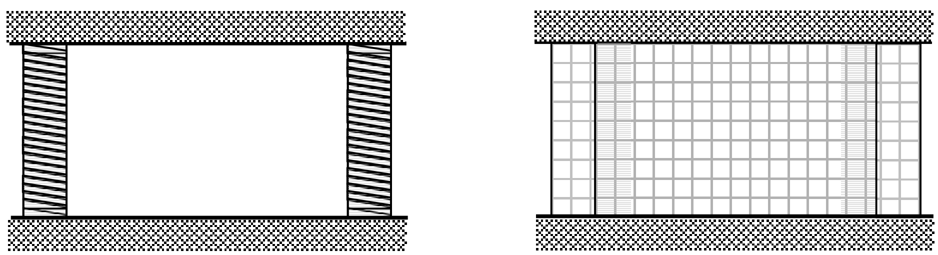

**(a) column** **(b) wall side**

**Figure 5: SRF specimen**

**Table 5 Material properties of sheet and belt**

| | Model | Thickness (mm) | Width (mm) | Tensile strength (MPa) | Modulus of elasticity (MPa) |
|---|---|---|---|---|---|
| Belt | SRF3050 | 3 | 50 | 532 | 2904 |
| Sheet | SRF905 | 0.9 | | 203 | 1355 |

## BASE MOTION INPUT PLAN AND INSTRUMENTATION

The two specimens were subjected to the series of recorded motions with selected five levels as shown in Table 6: TOH, Miyagi-ken Oki earthquake recorded at Tohoku university in 1978, ELC, Imperial Valley earthquake recorded at El centro in 1940, JMA, Hyogo-Ken Nambu earthquake recorded at Japan Meteorological Agency in 1995, CHI, Chile earthquake in 1985. The SRF specimen, which survived these motions, were subjected to additional three motions with higher levels of TAK, Hyogo-Ken Nambu earthquake recorded at Takatori station in 1995 and CHI, after removing the collapsed RC specimen from the table.

The levels of the base motions were determined on the basis of preliminary analysis results, from which the RC specimen was expected to collapse at the stage 5 (CHI50). The duration time of the base motions was scaled by $1/\sqrt{3}$ to satisfy the similitude law. The axial stresses and shear coefficients were also corresponded to the proto-type six-story building by the additional mass (steel plates) on the specimen.

Before and after the input of base motions, a white noise motions with small level was input to observe the change of the natural frequency of the damaged specimens.

**Table 6 Base motion input plan**

| Earthquake data | Maximum target velocity | Ratio to the prototype | Maximum acceleration of prototype | Maximum velocity of prototype | Maximum acceleration input to specimen | Maximum velocity input to specimen |
|---|---|---|---|---|---|---|
| | (kine) | | (gal) | (kine) | (gal) | (kine) |
| TOH** | 12.5 | 0.3 | 258.2 | 40.9 | 77.5 | 7.2 |
| TOH** | 25 | 0.6 | 258.2 | 40.9 | 155 | 14.4 |
| ELC** | 37.5 | 1.1 | 341.7 | 34.8 | 375.9 | 21.7 |
| JMA** | 50 | 0.6 | 820.6 | 85.4 | 492.4 | 28.9 |
| CHI** | 50 | 0.7 | 884.4 | 70.6 | 619 | 28.3 |
| TAK* | 125 | 1.0 | 605.5 | 124.2 | 605.5 | 71.6 |
| CHI* | 63 | 0.9 | 884.4 | 70.6 | 796 | 36.4 |
| CHI* | 50 | 0.7 | 884.4 | 70.6 | 619 | 28.3 |

** for the simultaneous test with the two specimens, * only for the SRF specimen

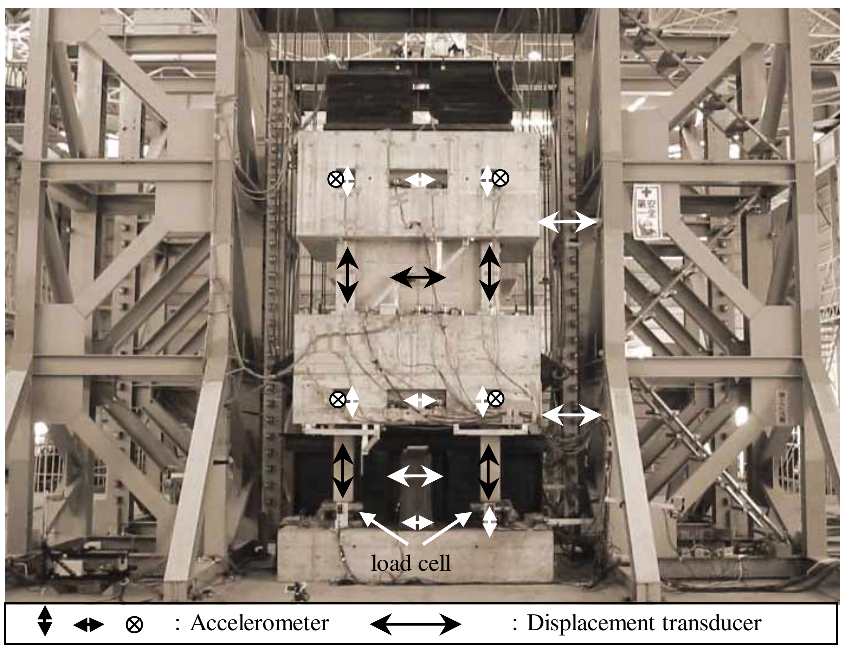


**Figure 6 Experimental setup and instrumentation**

The responses of the specimens to the base motion, such as acceleration, displacement, strain in steel bars and shear and axial forces in the first story columns, were recorded in 1000Hz sampling rate using accelerometers (22 channels), displacement transducers (20 channels), strain gauges (36 channels) and load cells (4 channels), respectively. The experimental setup and location of measuring instruments are identical for both specimens as shown in Figure 6. Also four different types of accelerometers were used for another objective, the development of economical and mass-productive accelerometers as standard tools for damage detective system or disaster prevention system. From the recorded accelerograms in each story, the maximum inter story drift can be calculated after the earthquake events, by which the warning during the earthquake or the post-earthquake safety evaluation can be done automatically.

## TEST RESULTS

### Damage process

The damage process of the specimens was evaluated by three methods, which were observation of cracks generated in specimen, the number of yielded strain gauge attached to reinforcing bars and the change of natural frequency calculated from system identification method. In case of the SRF specimen, however, the sheet and belt covering the surface of the specimen made it impossible to observe cracking, so only the two methods were available.

The numbers of yielded strains per measured in the steel bars are summarized in Table 7, which shows that all the longitudinal steel bars of both specimens were yielded at JMA50 and all the hoop reinforcements of the RC specimen were yielded at CHI50-1. The discrepancy in the numbers of yielded stain gauges between the two specimens also support the effectiveness of the SRF retrofit method.

The initial crack was occurred on the wall rather than on the column after TOH25, which was not expected and may be responsible for the out-of-plane deformation due to the torsional response. Furthermore, it was after JMA50 when the first crack was observed on the column, as though it is not explained considering the number of yielded strain gauge attached on the longitudinal steel bars.  The crack patterns developed on the columns and the wall after JMA50 is illustrated in Figure 7.

**Table 7  Number of yielded strain gauges**

| | Main bars | | Hoop | |
|---|---|---|---|---|
| | West column | East column | West column | East column |
| ELC37.5 | 0/8 (3/8) | 0/8 (2/8) | 0/7 (1/7) | 0/7 (0/7) |
| JMA50 | 8/8 (8/8) | 8/8 (8/8) | 0/7 (2/7) | 0/7 (0/7) |
| CHI50-1 | 8/8 (8/8) | 8/8 (8/8) | 1/7 (7/7) | 2/7 (7/7) |
| TAK125 | 8/8 | 8/8 | 1/7 | 3/7 |
| CHI63 | 8/8 | 8/8 | 6/7 | 6/7 |
| CHI50-2 | 8/8 | 8/8 | 6/7 | 6/7 |

( ): RC specimen

**Figure 7  Crack pattern developed in columns and wall after JMA50**

Due to the large inelastic displacement responses under CHI50-1, the reinforced concrete(RC) specimen failed in shear after yielding and simultaneously lost the axial load capacity. The RC specimen totally collapsed after twenty seconds during the input and fall down to the column side, and thereafter the gravity load on the column side was supported instead by the steel beam which had been set up under the bottom of the second floor mass for the protection of possible pancake collapse. Observed damages of the columns after CHI50-1 are compared as shown in Figure 8. Only slight damages at the column ends can be observed in the SRF specimen.

**(a) RC specimen** **(b) SRF specimen**

**Figure 8 Columns after CHI50-1**

**Stiffness deterioration**

The change of the natural frequency for both specimens in the course of damaging was computed using ARX model[5], from acceleration records at the base and on the concrete mass W2 under the white noise input. As shown in Figure 9, the natural frequencies for both specimens gradually decrease with increasing of damage developed in the specimens, where the higher decreasing rate can be observed in the RC specimen than in the SRF specimen.

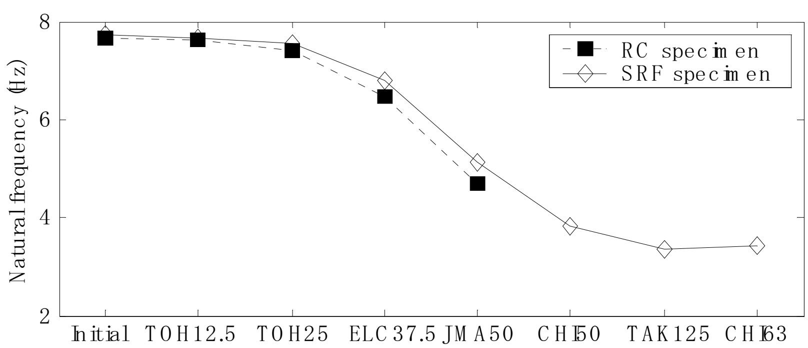


**Figure 9 Transition of natural frequency**

**Time-history responses**

Figure 10 shows time-history of the horizontal displacement responses of the wall and the column side during ELC37.5, which were recorded from the displacement transducer instrumented between the base and the bottom of W1. The horizontal displacement response of the column side was much larger than that of the wall side in both specimens, which resulted from the torsional response with considerable eccentricity. The similar responses were observed in the other input stages as though not presented here. Furthermore, the horizontal displacement responses of the RC specimen were slightly lager than those of the SRF specimen from TOH12.5 to JMA50 input, which became obvious in the first part of CHI50-1 input stage where the RC specimen was collapsed after 20 seconds, while the SRF specimen responded stably. The time-history waves of the measured displacement responses during CHI50-1 are compared for the two specimens as shown in Figure 11.

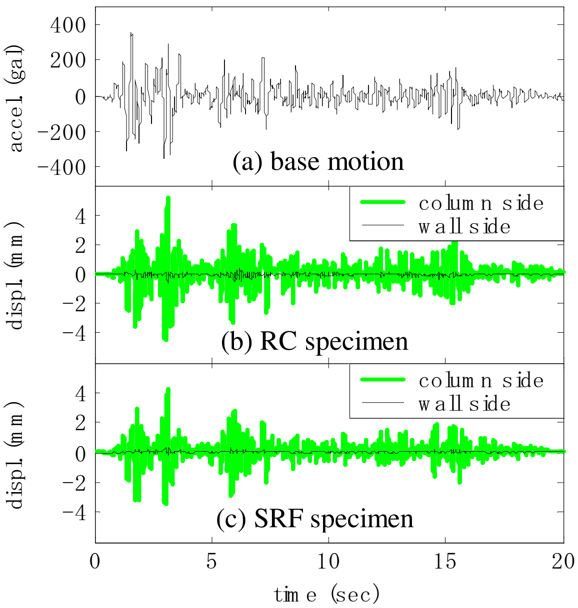


**Figure 10 Horizontal displacement during ELC37.5**

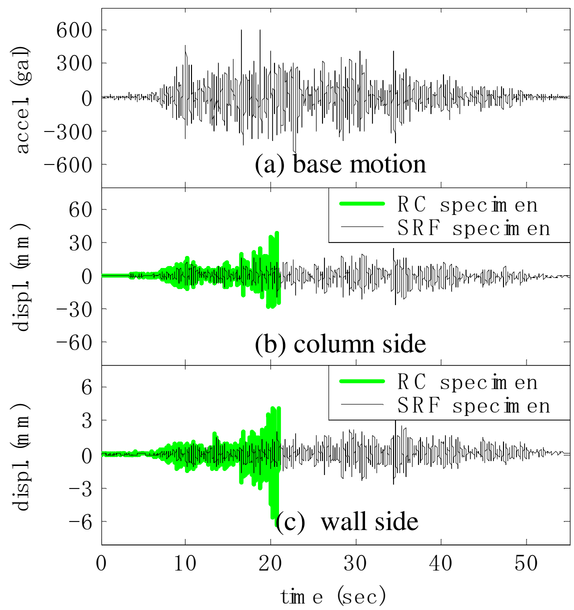


**Figure 11 Horizontal displacement during CHI50-1**

**Hysteresis relations**

The hysteresis relations between the horizontal displacement and the shear force in the two columns of the RC specimen and the SRF specimen are also compared in Figure 12. These shear forces are measured by the load-cells placed at the bottom of the two independent columns. Well-looking hysteretic relations can be obtained. It may be concluded that the axial and shear forces could be measured by these load-cells successfully. The vertical axis is the sum of the shear forces in the two columns of each specimens. The horizontal axis is the displacement response on the column side frame measured at the second floor or at the top of the first story columns. The values of the maximum and minimum shear force and displacement, for which and those from RC specimens are indicated as in parentheses. The solid and dotted lines are calculated shear strength (112.9KN) and shear at calculated flexural strength (125.5KN) respectively, for the two RC columns.

In TOH12.5 and TOH25, the hysteresis relations between two responses are almost linearly elastic. As the load level increases, the stiffness degrades and the lateral drift become larger, which is more obvious in RC specimen than in SRF one. The maximum shear forces were attained during JMA50 for both specimens, which was apparently larger in the SRF specimen than in the RC specimen. While the recorded maximum shear force in the RC specimen was almost the same as that of the calculated strength, that of SRF specimen exceeded that of calculated one, which may be due to the confinement of the SRF belts and the strain rate effect. In the RC specimen, it might be estimated that the strength decay in the shear resistance started to occur due to the obvious shear cracking during the response.

During the response to CHI50-1, the stiffness and strength degradations of the RC specimen became rapidly significant under the reversed cyclic loading and resulted in the shear and axial load collapse when the elapsed time was around 20 sec. On the other hand, the hysteresis relations of the SRF specimen showed stable behavior without strength decay, up to 24.5mm, corresponding to the rotation angle of 1/33 or 3/100.

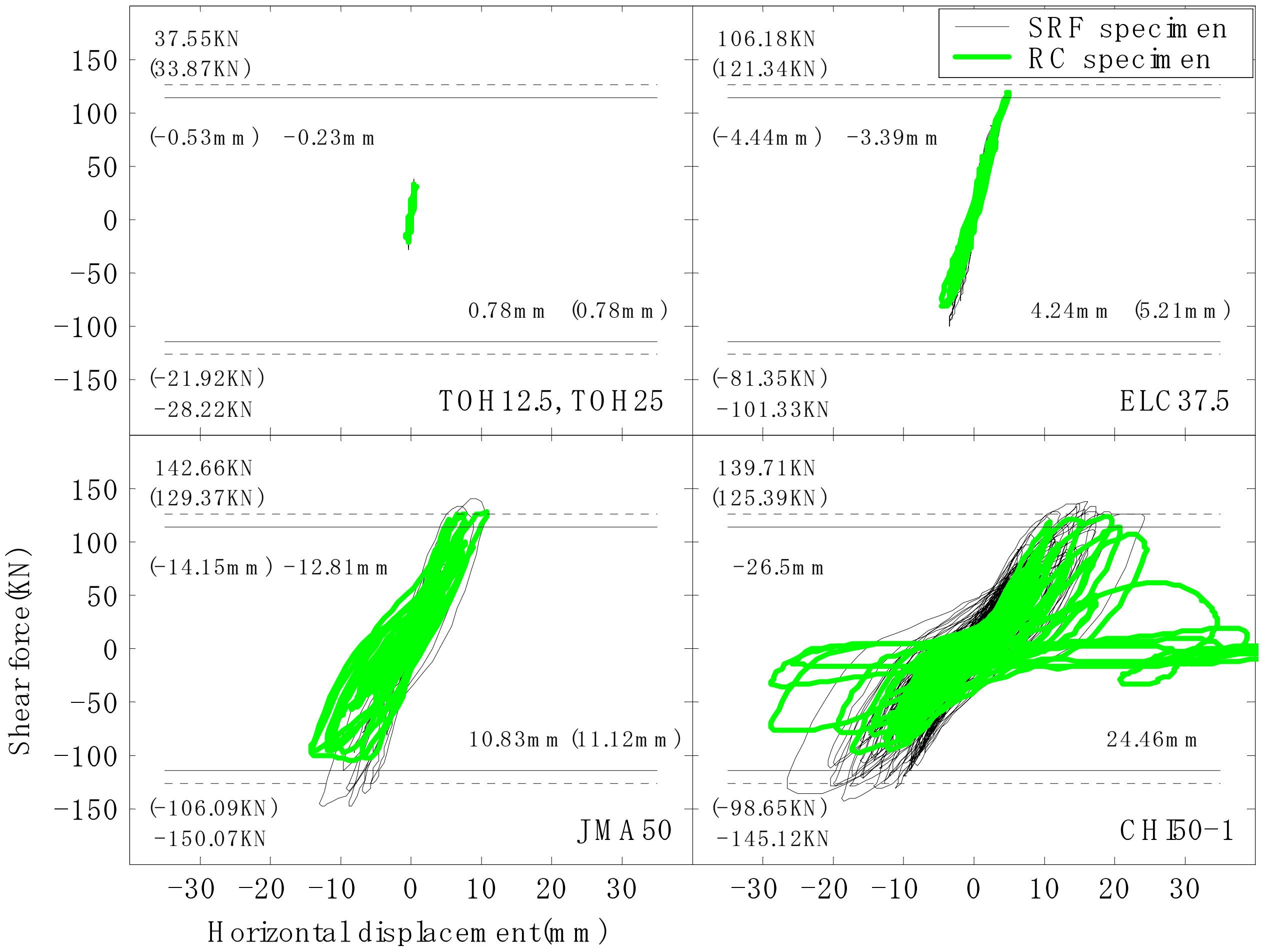


**Figure 12 Shear force and lateral displacement relations of the two columns**

**Hysteresis relations of SRF under higher motions**

After removing the collapsed RC specimen from the shake table, the SRF specimen was tested further under the three base motions with higher levels, TAK125, CHI63 and CHI50-2. Hysteresis relations between the shear force and the horizontal displacement of the columns during the responses to the succeeding motions are shown in Figure 13. Displacement response to the positive direction was accumulated because the same motion was input in the same direction. Therefore, relatively large residual displacements to the positive direction were generated after CHI63 and CHI50-2 due to these characteristics of the motions. Although the lateral stiffness and strength decayed, the SRF columns were stable against the axial collapse and survived these higher levels of the input motions even with disadvantages and severe conditions simulating succeeding or repeated occurrence of couples of major earthquakes. Even though the strength of the columns decayed during these test, the frame seemed to be stable: one of the reasons for the structural stability was estimated that the torsional strength and stiffness was effective as the resistance to the loading direction, because the damage to the wall was not fatal and the wall maintained not only translational but also torsional strength and stiffness of the structure.

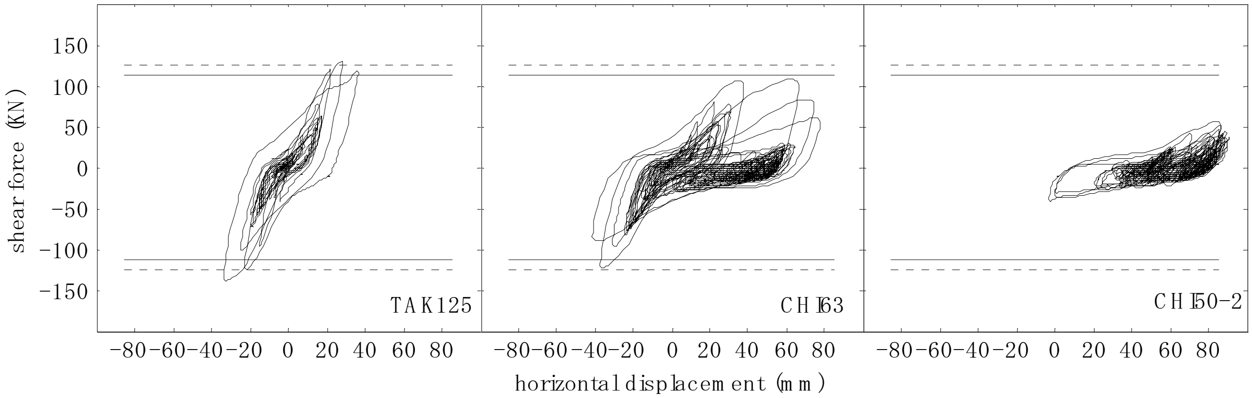


**Figure 13 Hysteresis relations of SRF specimen after the removal of the collapsed RC specimen.**

**Axial deformations of columns**

The measured axial deformations of each column in relations to the measured varying axial load are compared for the two specimens as shown in Figure 14 under the response to CHI50-1. It is observed that the axial load and axial deformation relations of the columns were not much different between the two specimens with larger tensile and slight compressive deformations, until the axial compressive deformation rapidly increases with the progress of the shear and failure in the RC specimen.

From the data of the hoop strains, the process and the cause of the axial failure in reinforced concrete columns may be interpreted as follows: The first peak of strength and drift induced critical cracking associated with yielding of the hoop and caused the residual hoop strains and the shear strength decay. The second peak exceeded the previous maximum, when the hoop might be ruptured, which induced the fatal loss of the interface shear resistance along the shear cracking and the axial capacity. It should be noted that the inelastic strain of the hoop after yielding accumulated with cyclic load which could be the main cause of the shear and axial failure of the column. On the other hand, in the SRF specimen, the sheet did not rupture and the passive confinement was effective until the end of testing.

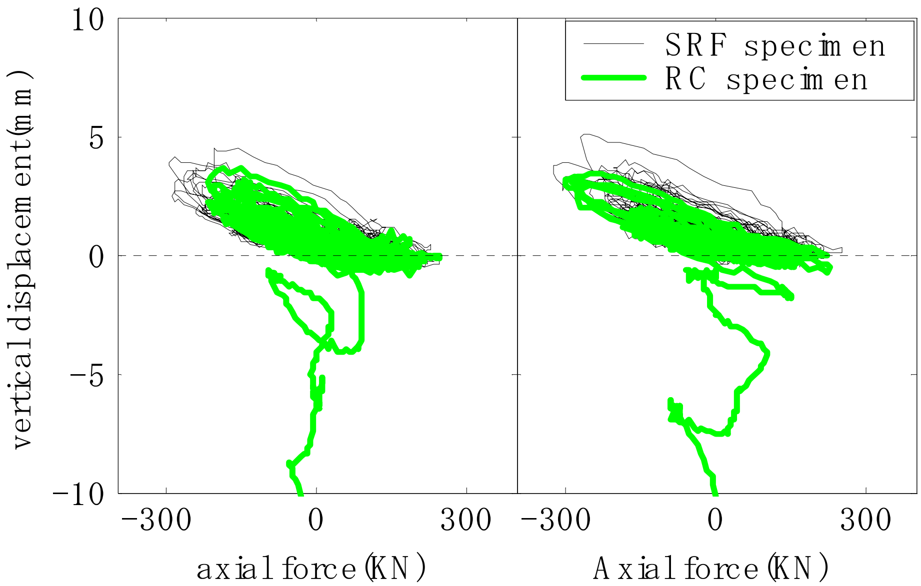


**Figure 14 Relations between axial force and axial deformation under CHI50-1**

After the removal of the RC specimen from the table, the axial load and the axial deformation relations of each column for the SRF specimen are also shown in Figure 15 during the responses to the succeeding input motions of higher levels: TAK125, CHI63 and CHI50-2. The axial compressive deformations were not obvious even under TAK125. Although the axial compressive deformation progressed gradually up to 20mm, the averaged axial strain of 2.5/100, due to the large numbers of cyclic load reversals under CHI63 and CHI50-2, the constant gravity load can stably sustained by the columns strengthened with SRF.

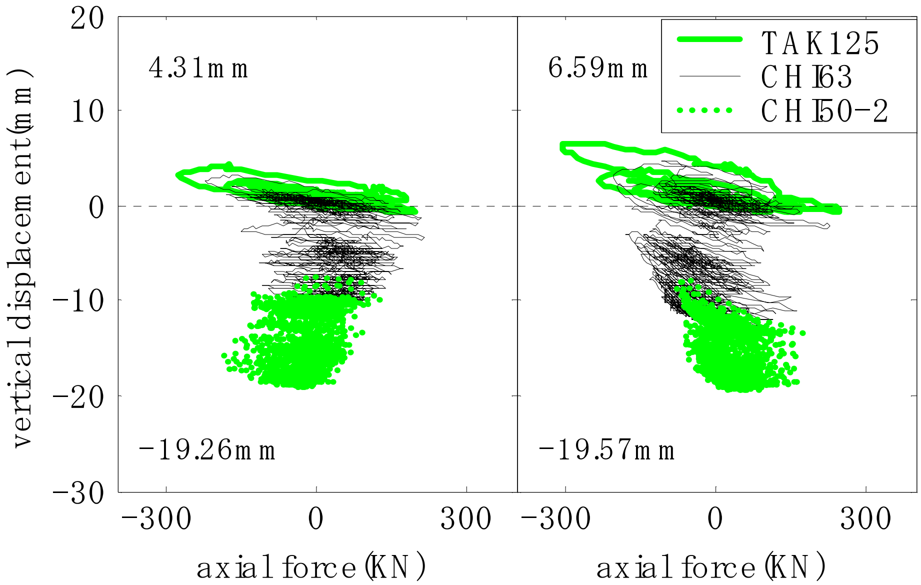


**Figure 15 Relations between axial force andaxial deformation of SRF specimen after the removal of the collapsed RC specimens**

## CONCLUSIONS

Two specimens with and without polyester sheet (SRF) strengthening for eccentric soft-first story were tested on the shaking table simultaneously. The following conclusions may be drawn from the results of the earthquake simulation tests.

The collapse process of reinforced concrete columns without strengthening was simulated by the dynamic test during responses to CHI50-1, which failed in shear and resulted in axial crushing due to inelastic lateral load reversals. On the other hand, the SRF specimen showed stable much stable behaviour with minor damage and without strength deterioration under the same earthquake motion. The strengthening method is proved to be effective not only against axial failure but also to damage control.

The SRF specimen survived succeeding three extreme earthquake motions by which fail-safe stability of the frame was verified. Although strength deterioration and axial deformations were observed during these tests, the seismic safety performance level of the original RC frame with poor detailing and unbalanced structural plan was amazingly improved by the SRF strengthening. The fail-safe toughness under excessive large deformation may be pointed out as an outstanding performance of SRF columns. The method is ready for widely use in practice, which will reduce the cost of retrofitting remarkably.

## ACKNOWLEDGEMENT

The test was carried out as a part of the research project "Development of post-earthquake performance evaluation using practical accelerometers," (Grant No. 12308018, PI: Toshimi Kabeyasawa) under the support of JSPS and Monbukagakusho. The dynamic test was conducted at NIED, Tsukuba, with Dr. Shun'ichi Igarashi, Square Inc., Dr. Nobuyuki Ogawa and Mr. Atsushi Kato, NIED. The support and the cooperative works for the tests are gratefully acknowledged. The strengthening method reported herein has been international patent pending as "SRF" method by Square Inc., Japan.

## REFERENCES

1. Kabeyasawa, T., Tasai, A., Igarashi, S., "A New Method of Strengthening Reinforced Concrete Columns against Axial Load Collapse during Major Earthquake," Proceedings of EASEC-8, CD-ROM, Singapore, 2001.

2. Kabeyasawa, T., Tasai, A., Igarashi, S., "An Economical and Efficient Method of Preventing Old Reinforced Concrete Buildings from Collapse under Major Earthquake," Proceedings of 7NCEE, CD-ROM in print, Boston, 2002.

3. Kabeyasawa, T., Kim, Y-S, et al, "Earthquake Simulation Test on Reinforced Concrete Buildings with Eccentric Soft-First Story, Part 1:Outline of Test and Part 2:Result of Test (in Japanese)," Proceedings of The Third Symposium on Improvement of Preparedness to Earthquake Disaster by Investigating Collapse Process of Structures, JSCE, 2002, 165-176.

4. Kabeyasawa, T., Tasai, A., Igarashi, S., "An Economical and Efficient Method of Strengthening Reinforced Concrete Columns against Axial Load Collapse during Major Earthquake," Proceedings of the Third Workshop on Performance-based Engineering on Reinforced Concrete Building Structures, 2001, pp. 371-384.

5. Erdal Safak (1991): Identification of Linear Structures Using Discrete-Time Filters, J. Struct. Eng. ASCE, Vol. 117(10), 3064-3085